

Finite Element Analysis of a Guideway for Automated Transit Networks

Isaac A. Gendler
San Jose State University
Professor Burford Furman
Davidson student scholar program
May 10, 2017

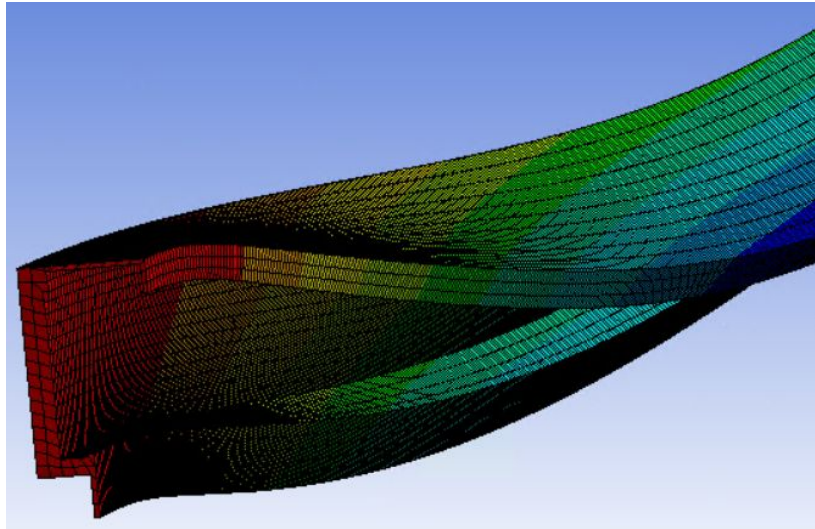


Table of contents

1. [Abstract](#)
2. [Introduction](#)
3. [Set up \(The guideway, loading\)](#)
4. [Methodology \(Finite element analysis, ANSYS, iteration based approach\)](#)
5. [Iterations \(Iteration 1 – Iteration 2, Iteration 3 – Iteration 4 - Iteration 5\)](#)
6. [Conclusion](#)
7. [Acknowledgements](#)
8. [Appendix](#)
9. [References](#)

Abstract

An asymmetric beam currently being utilized in a solar powered automated transit system was analyzed for its deflections, stresses, and angle of twist. Finite element analysis (FEA) with ANSYS was used in conjunction with hand calculations from beam theory to determine the response of the guideway to loading anticipated in normal operation. An iterative approach was used for modeling the system, where the geometry was taken from a simplified case and progressed in complexity until the original model was duplicated. After analysis, the deflections, stresses, and angles of twist were found to be within suitable ranges for a suspended transportation system.

1. Introduction

The structural performance of an asymmetric beam being used in a personal rapid transport system was computationally analyzed using finite element analysis. Finite element analysis can be performed on a variety of structures (Sachdeva et. al 2017), such as personal rapid transit (PRT) systems. A PRT system uses podcars, automated driverless vehicles to transport passengers on a guideway (Furman et al 2014). Finite Element Analysis (FEA) a modern software tool that is integral in the design process to help ensure that parts and structures will not fail under anticipated loading conditions. Since these guideways will be supporting a number of pod cars, the analysis will need to be done for the worst case scenario.

One such system is being developed at San Jose State University known as the Spartan Superway (Furman 2016) (**fig.2.1**). The Spartan Superway employs an elevated guideway (a beam which upholds the podcar) developed by Beamways Inc. (Gustafsson 2014) to serve as the framework for mobility. Before implementation, the structural elements of the asymmetric beam needs detailed FEA to be completed. After analysis, it was found that the deformations, stresses,

and twisting were in safe ranges for public transportation



Figure 2.1 The Spartan Superway system.

Full-Scale model of a section of the guideway, cross section used for analysis shown

2. Set up

2.1 The Guideway

The guideway being currently used by the Spartan Superway was developed by Bengt Gustafsson of Beamways PRT systems. The guideway is composed of 8 modular 3m long sections, each having 12 pegs, 6 insulators, 6 ribs, 5 debucklers, one side plate, two vertical bars, one lower stringer, one rail, and one ceiling. (fig. 2.23. (Gustafsson 2014) Due to its asymmetrical cross section, analytical methods are insufficient to accurately predict deflections, stresses, and twist. The dimensions are 520mm wide by 1000mm high by 24000mm long, and the modulus of elasticity for steel is 200000 N/mm^2

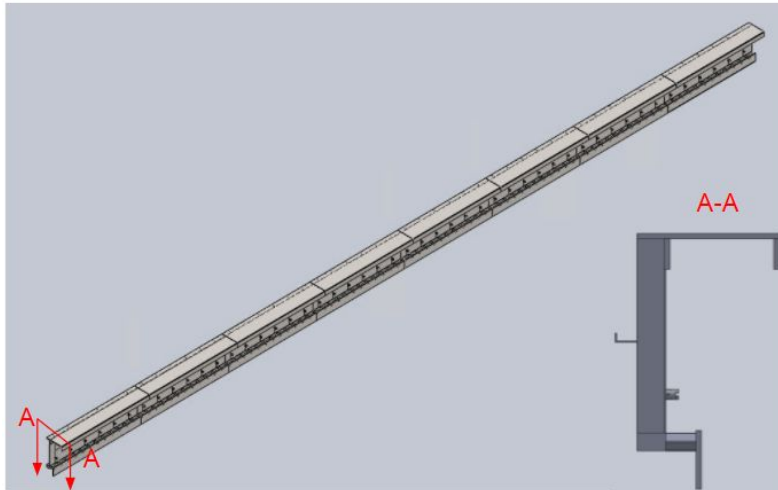


Figure 2.1 The Beamways guideway at isometric.
Section A-A represents the cross section

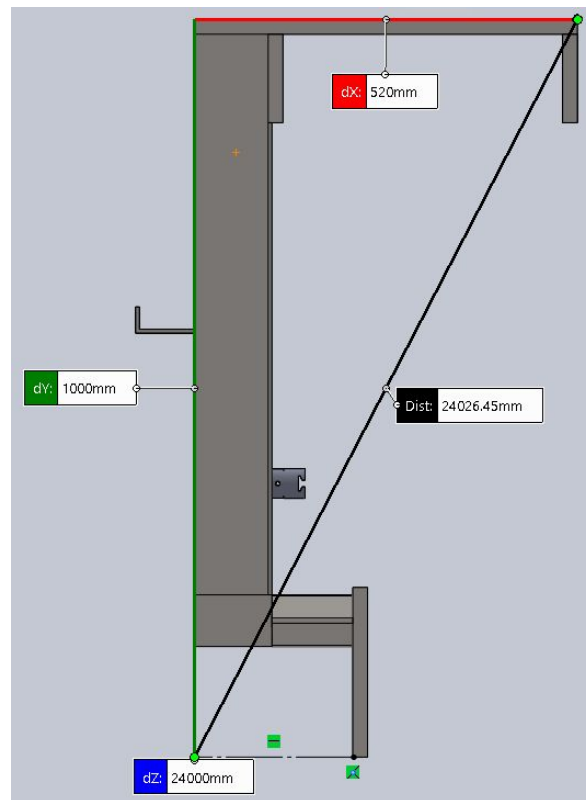


Figure 2.2 Profile of the Beamways guideway.
Dimensions are included

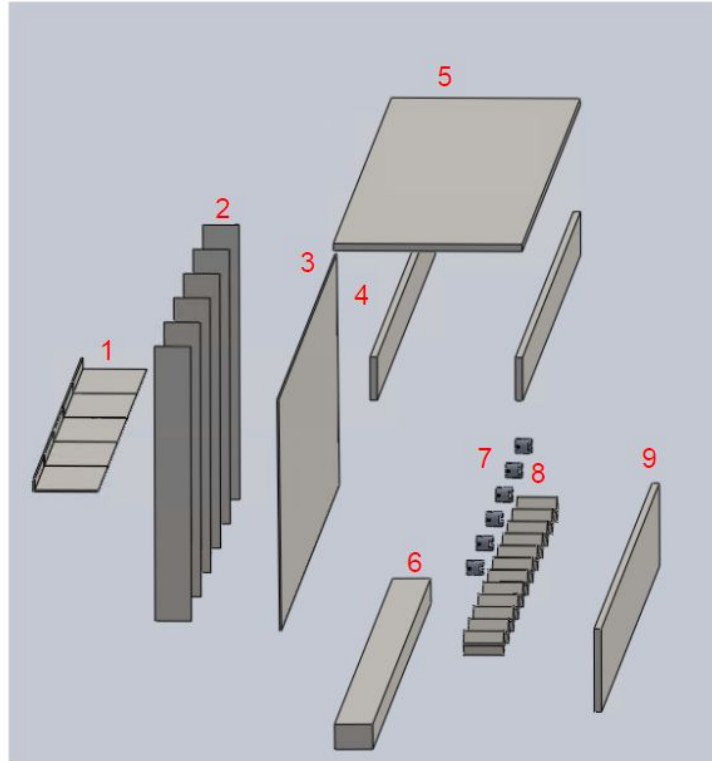


Figure 2.3 Exploded view of the guideway.
Parts in increasing order from left to right: (1) debucklers, (2) ribs, (3) side plate, (4) vertical bar, (5) ceiling (6) lower stringer (7) insulator (8) stud (9) rail

2.2 Loading

The guideway must be designed to withstand its own worst-case loading scenario. Such conditions will occur when the guideway encounters a heavy wind force while withstanding stationary podcar vehicles at maximum capacity are stacked nose to tail. Numerical analysis (Appendix A) establishes that the bogie would be experiencing a relatively large lateral wind force of 1981 N on its wheels to the upper side wall. and 3130 N to the outer lower side of the running surface flange where the switching wheels engage. The rest of the wind pressure of 306 Pascals would act directly on the outer part of the upper guide wheel running surface flange., and the weight of the bogie wheels would induce 5396 N of force every 1.5 meters. **(fig 2.4)** (Gustafsson 2016).

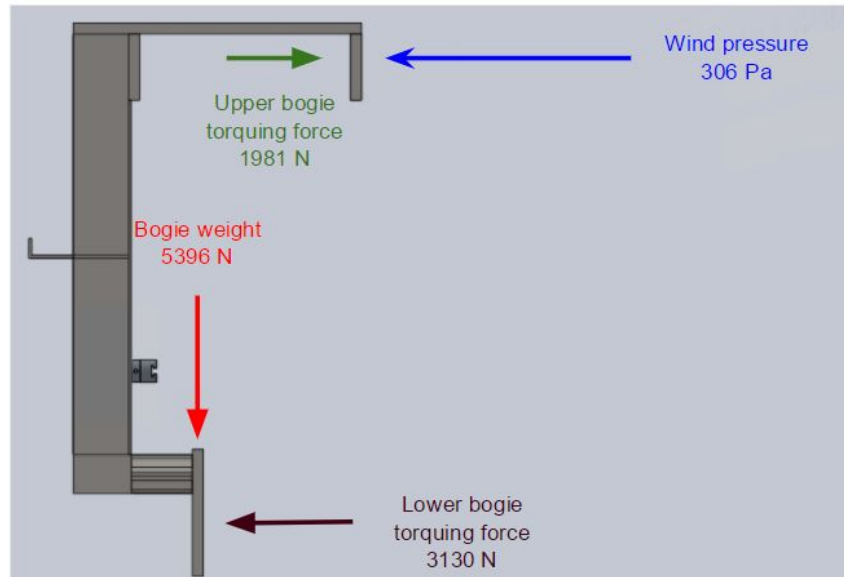


Figure 2.4 - Outline of the force assumptions.
Each arrow represents a force with magnitude

3. Methodology

3.1 Finite element analysis

FEA is a modern computer simulation tool that uses numerical methods to solve engineering problems that have no existing analytic solution and/or if the cost of experimental testing is too prohibitive. FEA works by discretizing a Computer Aided Design (CAD) geometry into a multitude of discrete “elements” to be connected at “nodes” (geometric edges) to create a “mesh”(Fig 3.1). The object is then to be acted upon by “governing equations” and “boundary conditions”. Governing equations describe and relate how the physics of a model interacts within its own structure (Bhavikatti 2014)) (for example, Hooke’s law, $F = kx$ is a governing equation that describes how a spring system works) to solve for field variables (the dependent variables of interests) while the boundary conditions specify the values of the boundary field variables (such as the supports for the aforementioned spring). In this system, the governing equations will be those applied to static cases (such as stress is equal to force divided by area, $\sigma = \frac{F}{A}$) the field variables would be the deformation and stresses, and the boundary conditions would be the supports used. Finite element analysis goes through three stages;

(i) The Pre-processing phase, in which the material properties, geometry, meshing (elements and nodes), loads, and boundary conditions are specified.

(ii) The Solution phase, in which all of the variables are interrelated to solve the field variables

(iii) The Post-processing phase, in which the values for the solution will be displayed

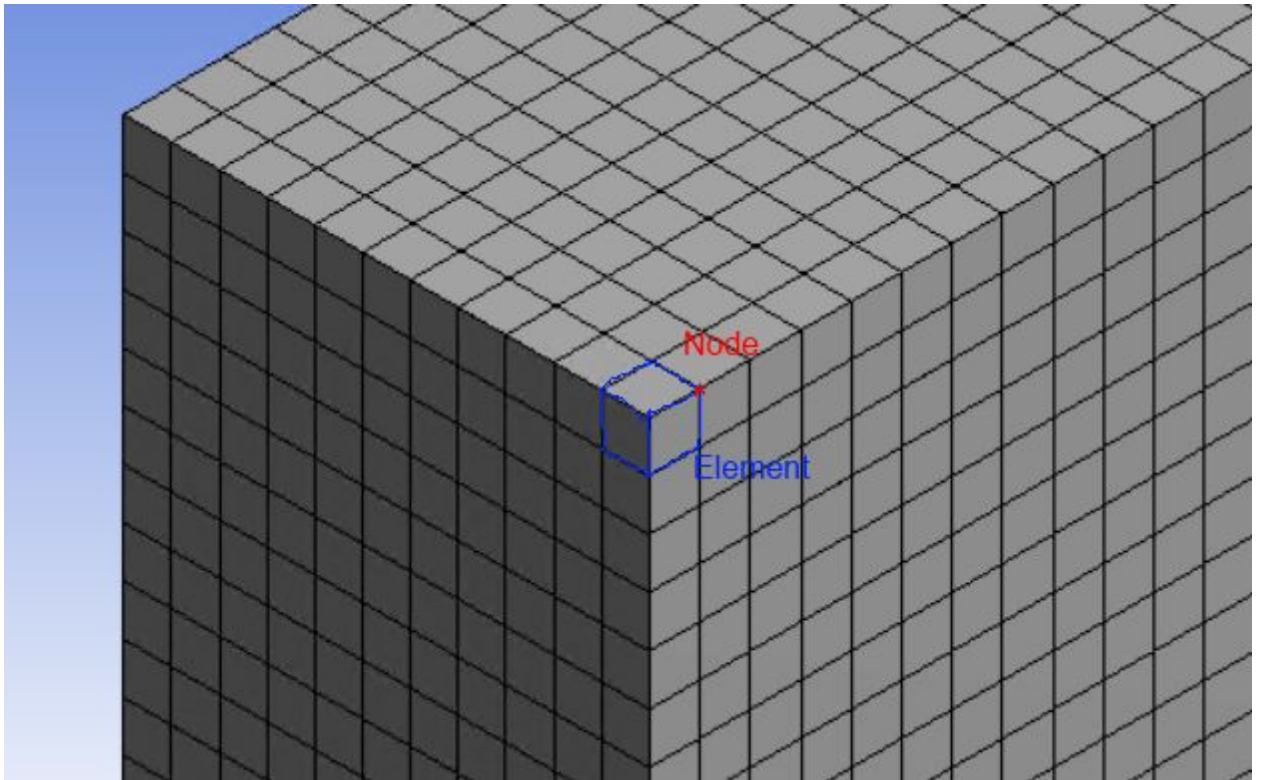


Figure 3.1 Nodes and elements

3.2 ANSYS

To perform FEA, a software package must be used. One such package is known as ANSYS. ANSYS has been used by many users, ranging from academicians researching structural engineering (Hua, X. G, et.al. 2007) (Husain Al-Sherrawi et. al 2014) to engineers working on offshore wind turbines (Sahroni 2015), and even the yacht team of Team New Zealand (ANSYS 2013). After post processing, the selected field variables (such as deformation or stresses) will be displayed visually on the elements, with each color corresponding to a range of values, all of which can be changed at the user's discretion (**fig 3.2**)

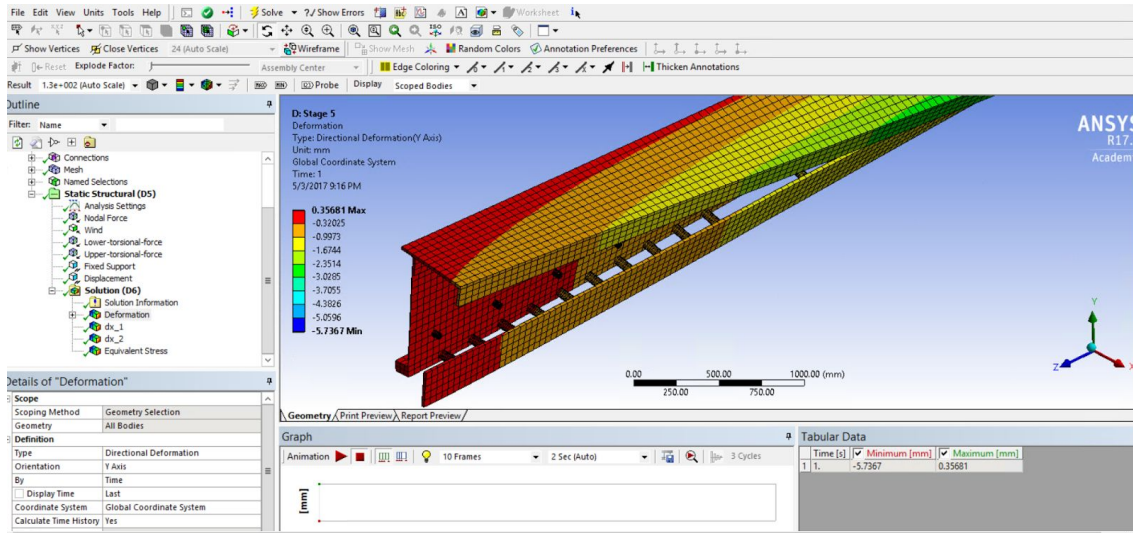


Figure 3.2 View of ANSYS

Display of deformation post processing values. Each element color corresponds to a range of possible values, as dictated by the bar to the left of the object. The minimum value of the color depends on the lowest value of it's box on the bar, while the maximum value is with its highest

3.3 Iteration based approached

Since FEA must be used carefully on models in which no known analytic solution is present (as verification of any results could only be done with approximations), the project was divided into five iterations. The first iteration began with a simple loading situation on a beam approximated by a rectangular solid bar geometry whose dimensions reflected the parameters of the beamway guideway profile. For the next three iterations, the geometry was given refined characteristics to produce a greater resemblance to the guideway, leading up to the fifth and final iteration, in which the original model was used. To illustrate the advantage, think of a sculptor and a stone tablet. Before the final image can be realized, the artist must start with a block that contains sufficient parameters, and must then carve said block, incrementing the design until the work has been perfected (**fig 3.3**). For all iterations, a mesh size of one node for every 50 mm was applied

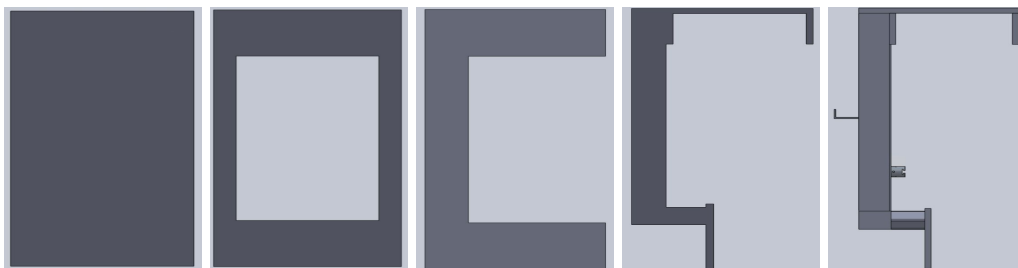
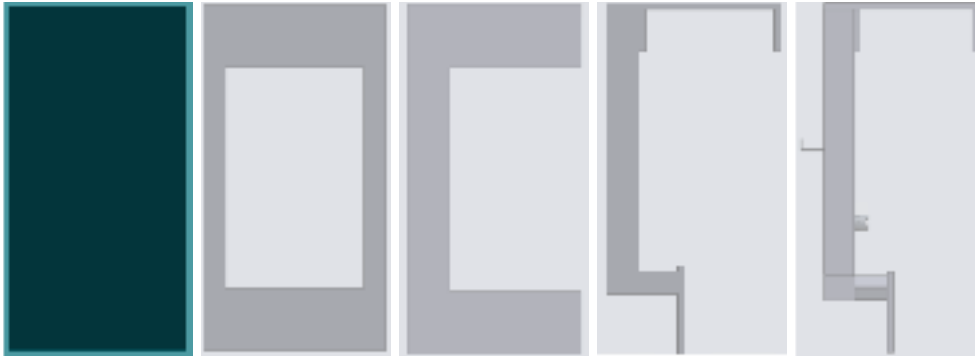


Figure 3.3: Cross sections used in successive iterations of analysis. From left to right: Solid rectangular profile, Hollow rectangular profile, C profile, G cross section, final profile

4. Analysis Iterations

4.1 Iteration 1 Solid rectangular profile



The first iteration (a bar with a solid rectangular cross section) can be seen in (fig.4.2). The dimensions of the profile were based off the extremities of the original model, 520mmx1000mmx24000mm (fig 4.3). Simple supports (constraining the front end to one translational degree of freedom and the back end to two and were used for the simulation, taken to be at the bottom edge of profile (fig 4.2) and all of the bogie forces were combined into a single central load of 80940 N which was used to simplify simulation. The wind and torque forces were not simulated since the geometry was deemed too simple. To verify the results from ANSYS, the linear deflection in the y-axis at the midspan can be predicted using the equation (fig 4.1)

$$d = \frac{5PL^3}{384EI} \quad (1)$$

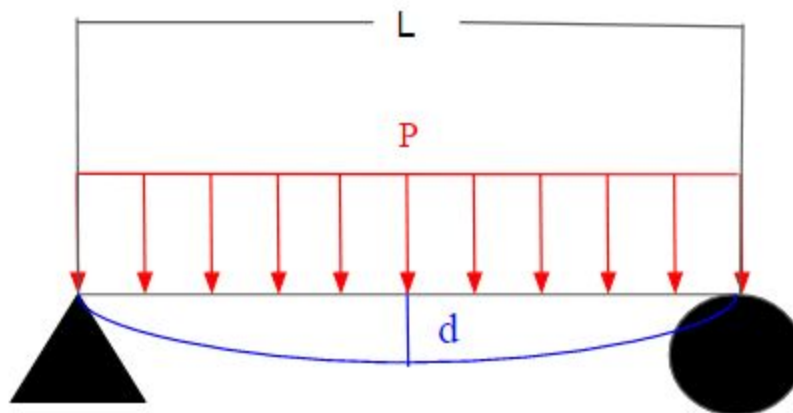


Figure 4.1 Diagram of loading
The linear load P acts over the entire length L to produce a deformation d

With P being the linear pressure loading (since the force in ANSYS was applied to a rectangular face, it was treated as a linear pressure for modeling), ($\frac{80940N}{24000mm} \rightarrow 3.37 N/mm$), L being the length ($24000 mm$), E being the modulus of elasticity ($200000 N/mm$), and I being the area moment of inertia (being equal to $\frac{bh^3}{12} \rightarrow \frac{520mm*(1000mm)^3}{12} \rightarrow 4.33 * 10^{10}mm^4$). After hand calculations, the deflection results came out to be equal to $1.68 mm$ (**fig 4.4**). Through ANSYS calculation, the final result came out to be $1.69mm$, within 0.6% of the prediction. The von-Misses stress for the system at midspan can be calculated with the equation

$$\sigma = \frac{PL^2}{8S} \quad (2)$$

with S being the section modulus ($\frac{bh^2}{6} \rightarrow \frac{520mm*1000mm^2}{6} \rightarrow 86666666.67 mm^3$) coming out to be $2.8 Mpa$. With an ANSYS simulation, the stresses at midspan analyzed to be $2.795 Mpa$ (**fig 4.5**). (Note: It is the second from the top value not the top that must be read for stresses, since the “red” zone encompasses the minimum possible discretized value to the maximum). A difference from the analytic solution of around 1.8% No twisting was observed.

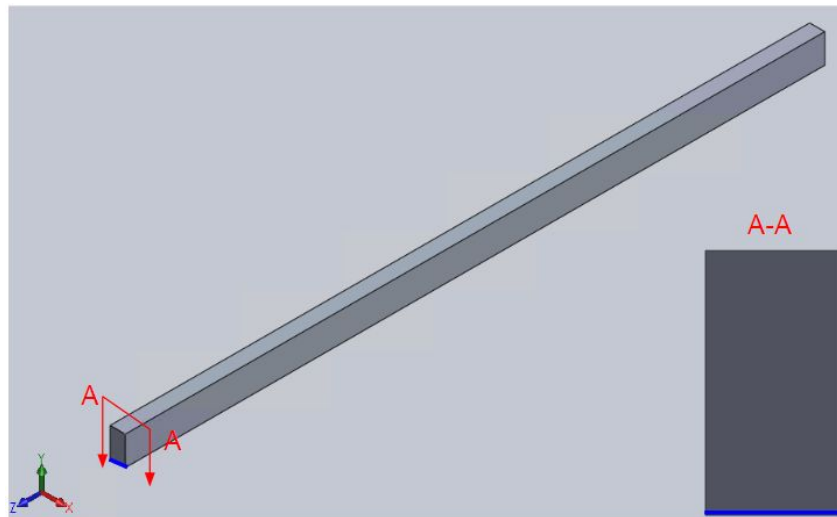


Figure 4.2 The first iteration at isometric.

Profile indicated by section AA. Fixed Supports applied at blue line on front face, while displacement (all rotations fixed and x and y translations fixed) applied on the same line in the rear face.

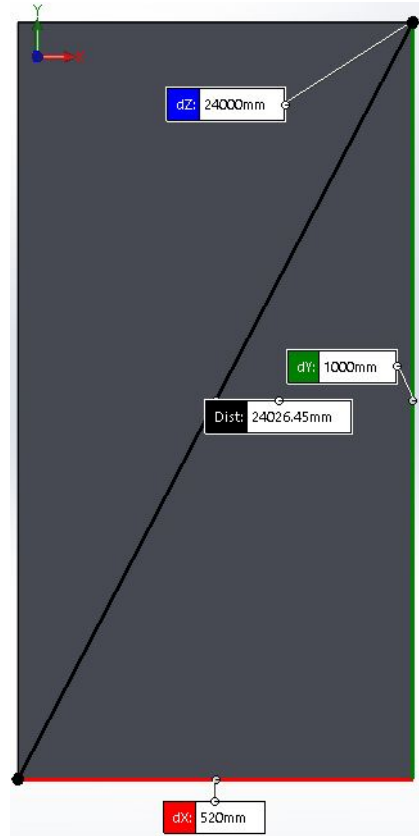


Figure 4.3 The profile of the first iteration with dimensions base b is outlined in red, height h in green

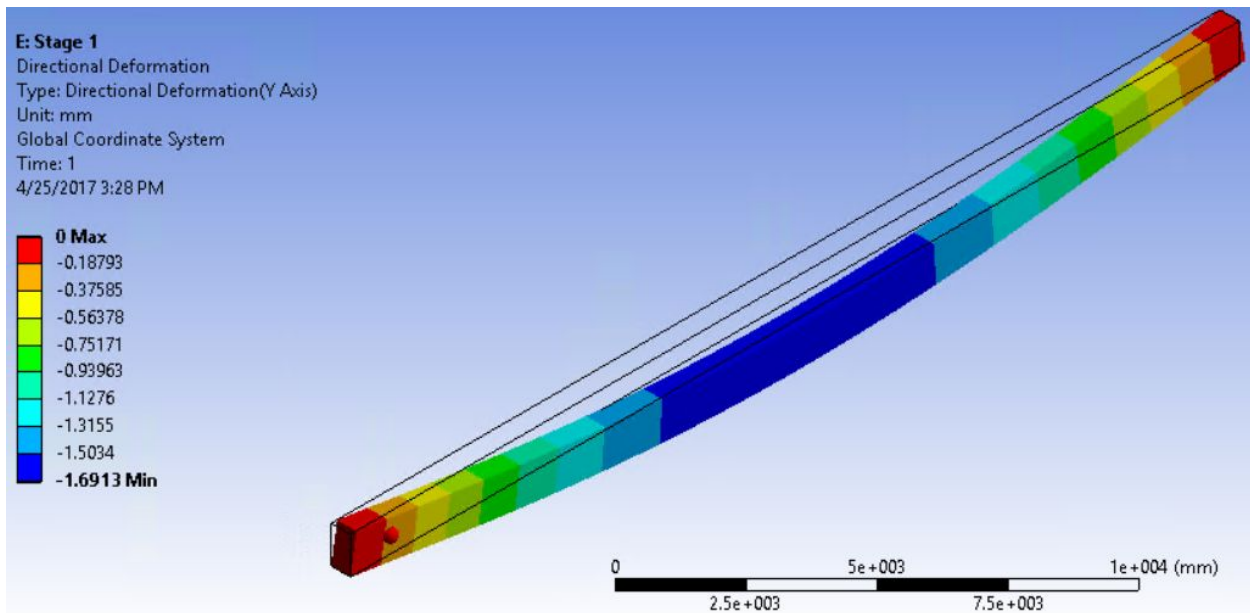


Figure 4.4 Iteration 1 deflection results
Regions of higher deformation are indicated by colors closer to blue on the color scale

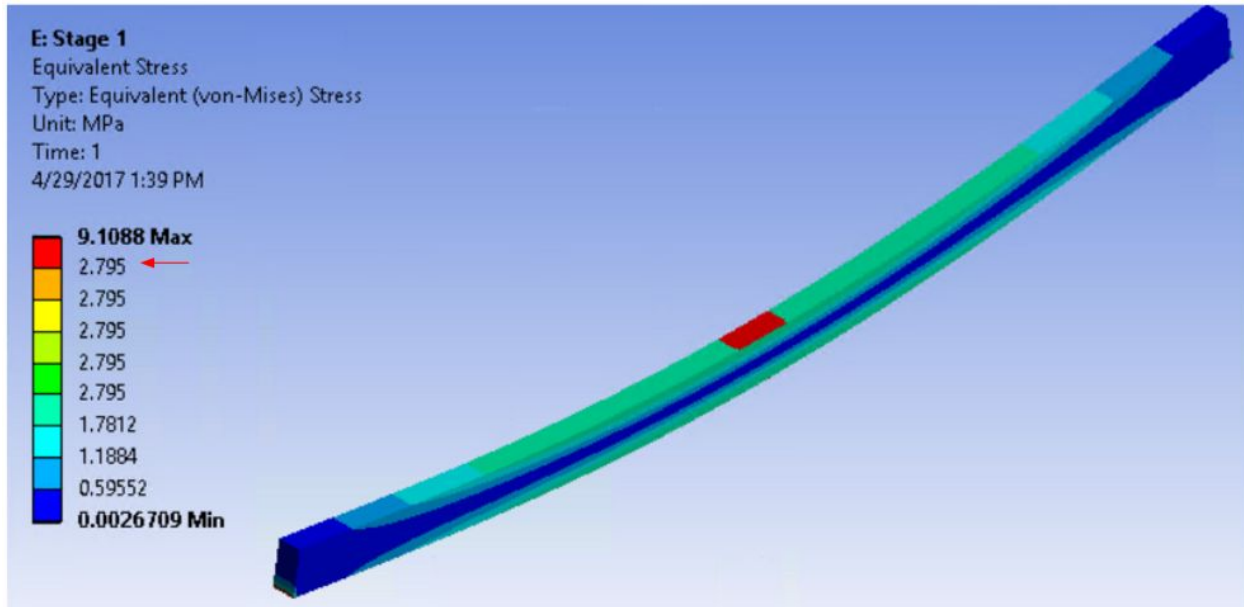


Figure 4.5 Iteration 1 stress results
The value for the red are in the middle corresponds to the value at which the red arrow is pointing

5.2 Iteration 2 Hollow rectangular profile



Since the beam is not perfectly solid but contains gaps, a logical step would be to incorporate a hole into the second iteration. The dimensions for said hole were based upon the area encapsulated between the top vertical bars and the lower horizontal bar (**fig 4.7**), due to its easy to find and symmetric nature. The profile for the iteration was then modified accordingly (**fig. 4.8**), giving it a moment of inertia

$$I = I_{outer} - I_{inner} = \frac{520mm \cdot (1000mm)^3}{12} - \frac{395mm \cdot (640mm)^3}{12} = 34.7 \cdot 10^{10} mm^4$$

and a section modulus

$$S = \frac{b_{larger}(h_{larger})^3 - b_{smaller}(h_{smaller})^3}{6h_{larger}} = \frac{520mm(1000mm)^3 - 395mm(640mm)^3}{6(1000mm)} = 6.94 \cdot 10^7 mm^3$$

Material properties were kept the same. Using equation (1) for deformation and equation (2) for stresses, 2.10 mm and 3.5 Mpa were predicted respectively. The vertical deformation was 2.13 mm, which was within 1.4% of the predicted value (**fig 4.9**). The von-Mises stress near the midpoint was 3.48 Mpa, a 0.57% error (**fig 4.10**)

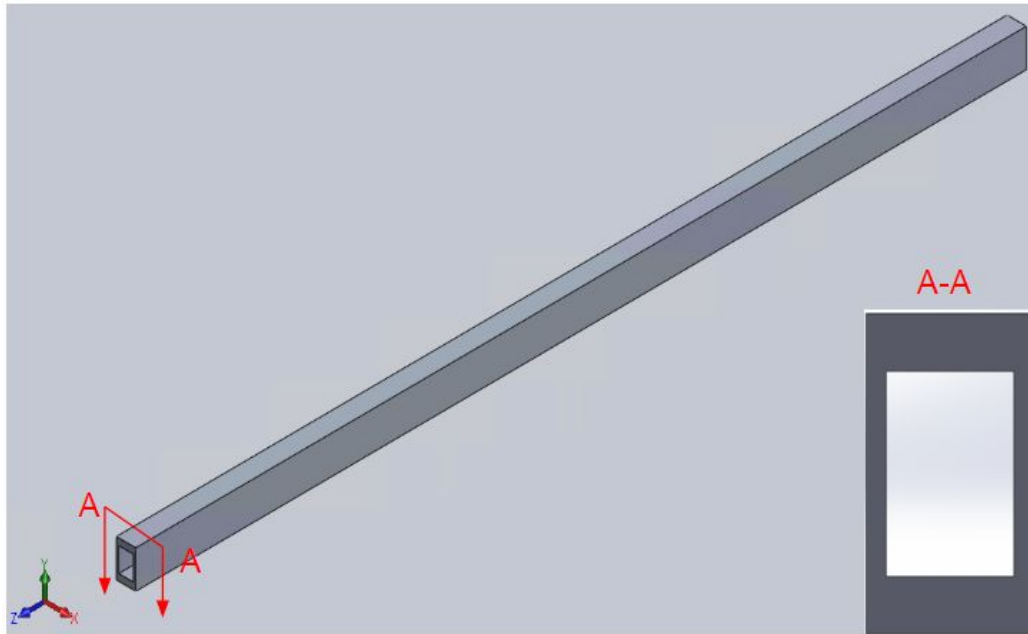


Figure 4.6 Second iteration - hollow rectangular cross section. This analysis was based on a hollow rectangular section with wall dimensions as shown the inset

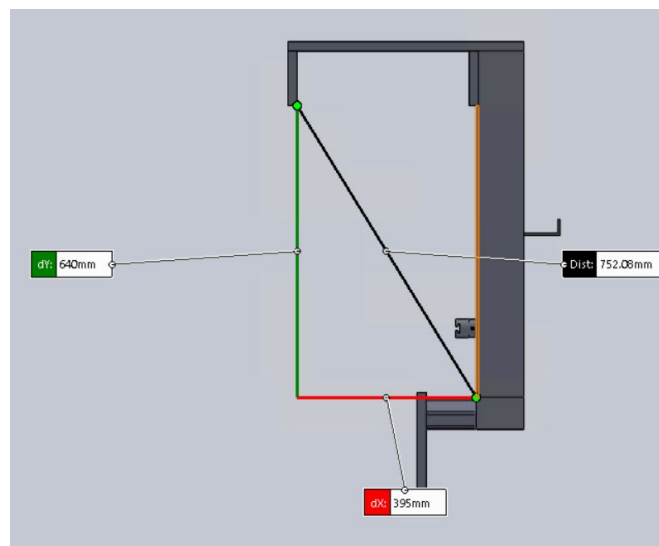
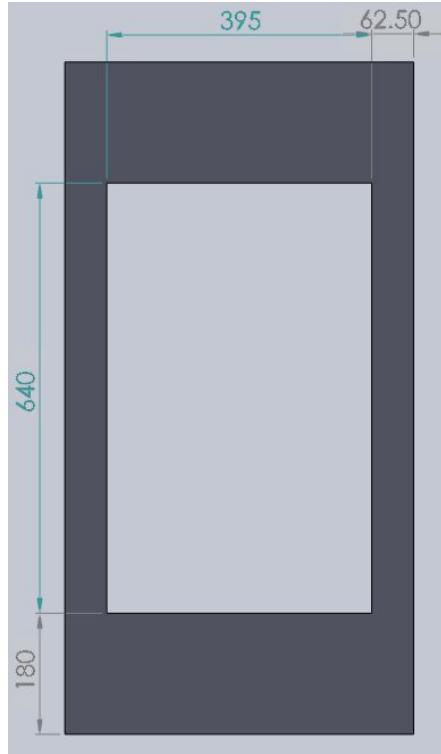


Figure 4.7 Dimensions of the hole used.
Base is 395mm, height is 640mm



**Figure 4.8 Profile of the second iteration
Dimensions (in mm) of hole in relation to the rest
of the profile included**

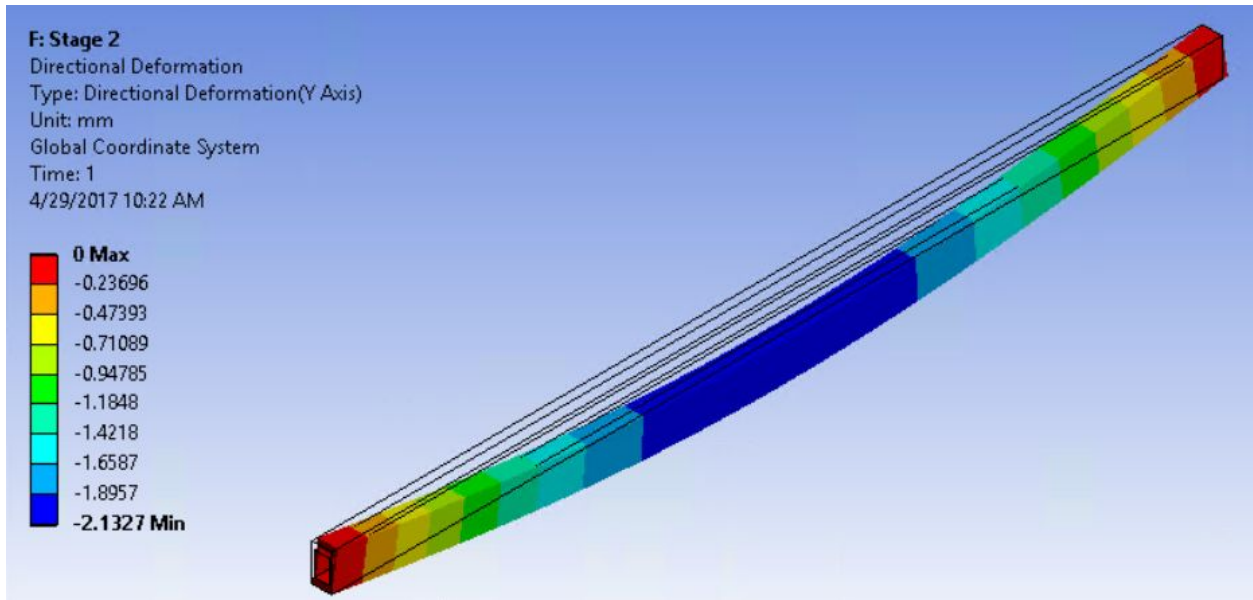


Figure 4.9 Iteration 2 deflection results

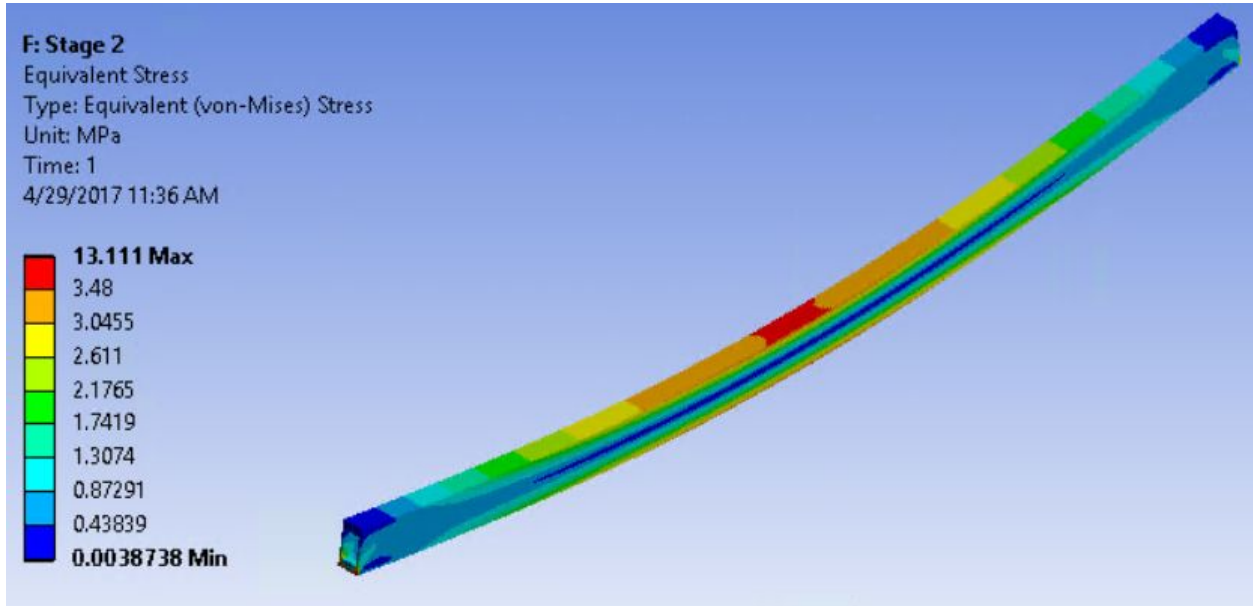
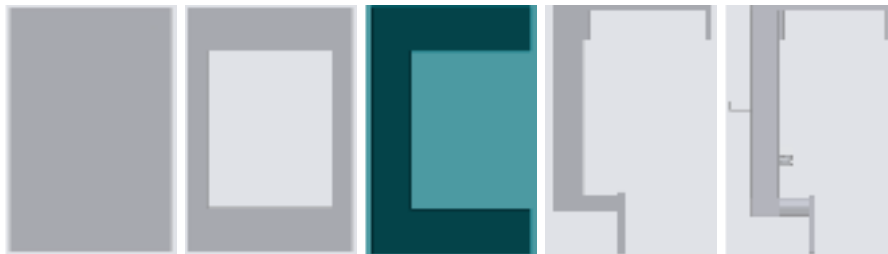


Figure 4.10 Iteration 2 von-Mises stress results

5.3 Iteration 3 The C profile



Since the the Beamways beam profile does not contain a centric hole, the next iteration should reflect that. As such, the gap was moved to the right to transform the beam into a “C” geometry (**fig 4.12**). The previous loading and support scheme was kept. The new moment of inertia around the x-axis can be calculated using the equation

$$I = \frac{(h-t_1)^3 t_2}{12} + 2 \left[\frac{bt_1^3}{12} + bt_1 \left(\frac{h-t_1}{2} \right)^2 \right] \quad (3)$$

with h being the height (1000mm), b being the base (520mm) t_1 being the thickness of the top and bottom pieces (180mm), and t_2 being the thickness of the centerpiece of the C beam(125 mm), resulting in a moment of inertia equivalent to around $2.82 * 10^{10} mm^4$, while the section modulus S is equivalent to $\frac{I}{h/2} \rightarrow \frac{2.82 * 10^{10} mm^4}{1000mm/2} \rightarrow 5.64 * 10^7 mm^3$. After plugging these values into equations (1) and (2), answers of 2.10 mm and 0.04 Mpa were arrived at respectively. ANSYS simulations reported around 2.49 mm (**fig 4.13**) for deflection and 3.0 MPa for stresses (**fig. 4.14**), resulting in error values of 18.6% and 7400% respectively.

Since the beam was not perfectly symmetric around the y-axis and the force was not placed at the shear center, twisting had occurred in the model. As such, it would only be natural to study it. The angle of twist for a particular geometry can be found using the equation

$$\theta = \frac{dx_2 - dx_1}{L} \quad (4)$$

Where dx_2 is the displacement of the top element of a linear geometry from the x-axis, dx_1 is the displacement of the bottom element of a linear geometry from the x-axis, and L (1000mm in this case) is the distance between them. **(fig. 4.15)** Data was collected from the ANSYS model through analyzing the x axis displacement from each node corresponding to dx_2 and dx_1 across the the z-axis path, plugging it into equation (4) and then graphing **(fig 4.16)** From this, it can be observed that a maximum twist of $5.76 * 10^{-4}$ radians occurs at midspan w, forming a parabolic structure. Since there was a slightly different number of elements between dx1 and dx2, the data for the first 10 results is uncorrelated and may be ignored.

Since the loading was not going through the shear center, analytic solutions will not be available. From now on only ANSYS simulations will be used.

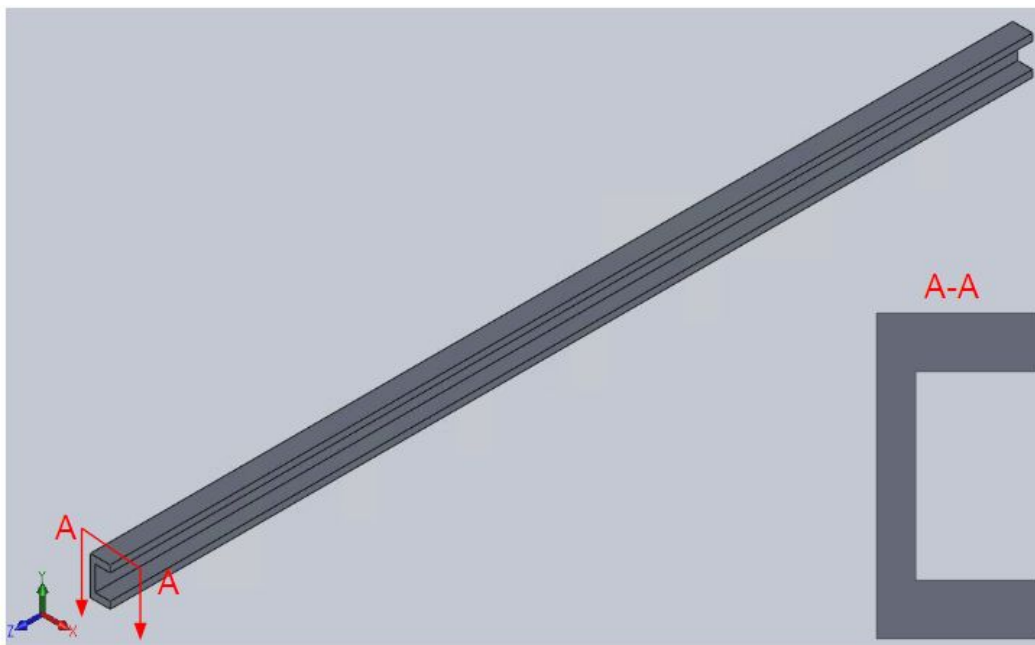


Figure 4.11 Iteration 3 isometric

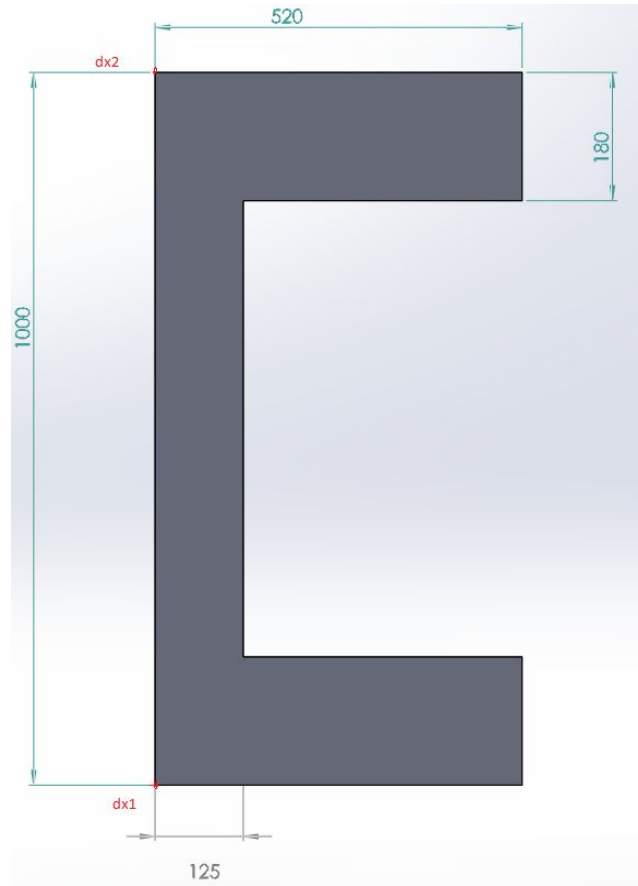


Figure 4.12 Iteration 3 profile
 Dimensions of the profile for iteration 3 are shown in the figure

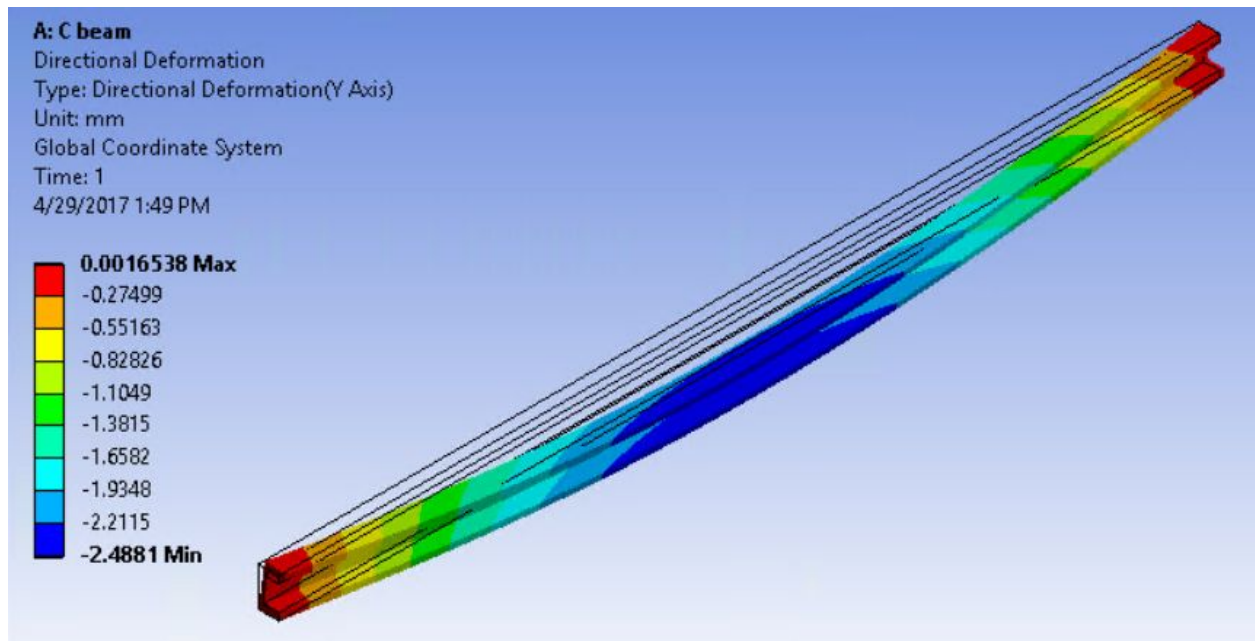


Figure 4.13 Iteration 3 deflection results
 Deflections are curved due to twisting

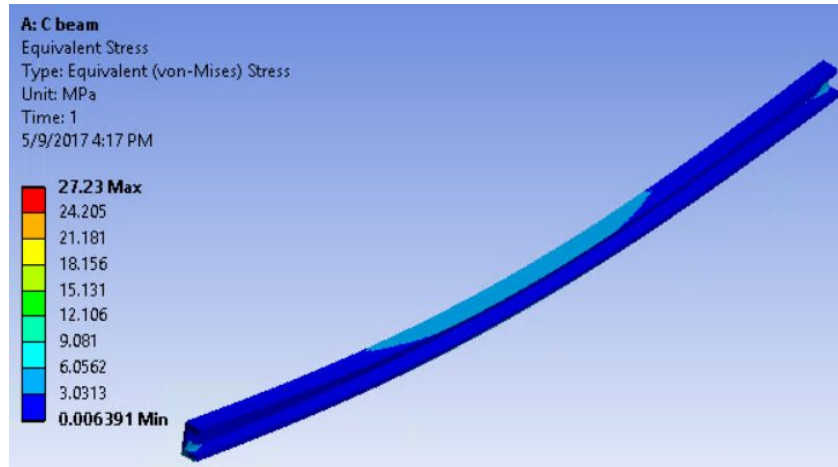


Figure 4.14 Iteration 3 stress results

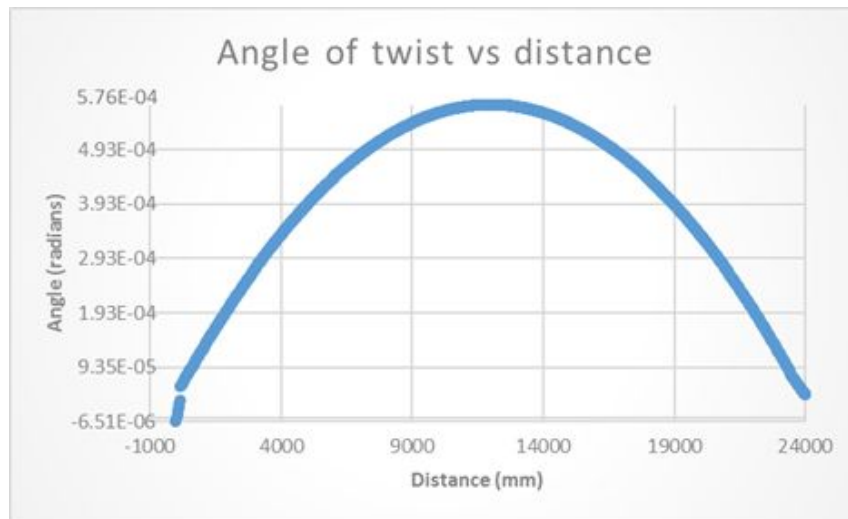
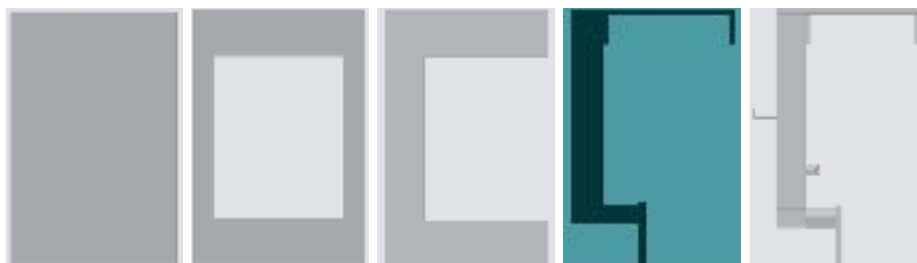


Figure 4.15 Measure of twist around axis Z for iteration 3. Max twisting occurs near the center of the beam length. The discontinuity near the beginning is a result of a different number of elements between the two paths.

5.4 Iteration 4 The G profile



The next iteration was to make the geometry like an idealized version of the beamway profile. The new profile was made to be a uniform version of the original guideway (**fig 4.17**). The lower edges of the profile were chosen for simple supports (**fig 4.16**) Because the geometry

of this model had a high similarity to the original version, it was decided to change the loading schematic to more accurately resemble the initials parameters (1981 N of the force through its wheels to the left chamber wall, 3130N to the outer lower railing, and a bogie weight every 5396N every 1.5 meters with a wind force of 306 Pascals on the top railing.(**fig 4.18**)). After ANSYS analysis, the deformation came out to be around 0.73 mm, (**fig 4.19**), the stresses 0.008 Mpa at mid center (**fig 4.20**) and the max twisting to be $3.34 * 10^{-4}$ radians, occurring near midspan (L was equal to 757 mm for three significant figures rounding) (**fig 4.21**)



Figure 4.16 Isometric of the fourth iteration. Edges outlined in blue were used for support placements.

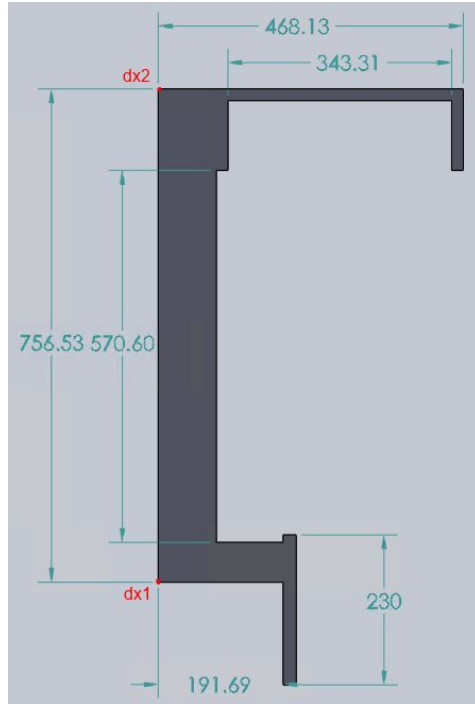


Figure 4.17 Profile of the fourth iteration. dx1 and dx2 are shown. Profile indicated by section AA. Fixed Supports applied at blue line on front face, while a displacement (all rotations fixed and x and y translations fixed) applied on the same line in the rear face.

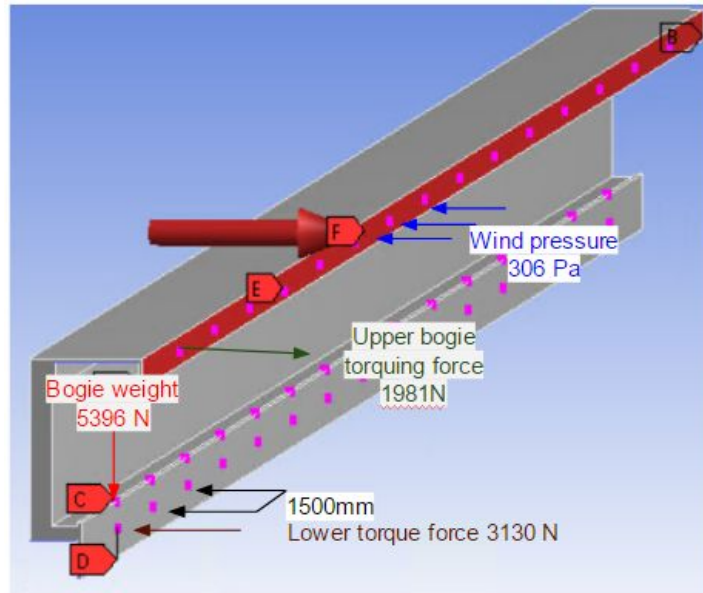


Figure 4.18 Force placement layout for iteration 4
Forces repeat every 1500 mm

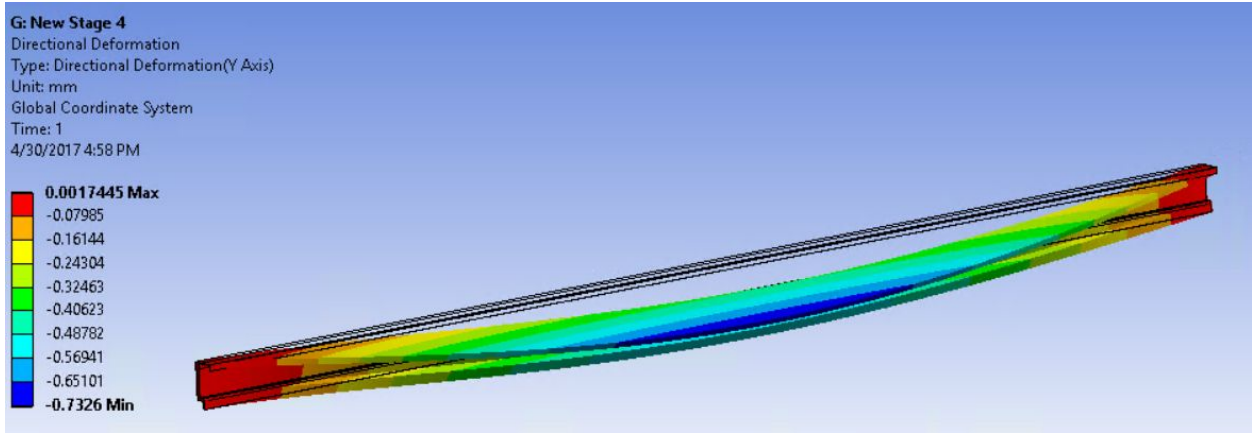


Figure 4.19 Iteration 4 deflection results
 Max deflection takes place at the upper surface flange at midspan

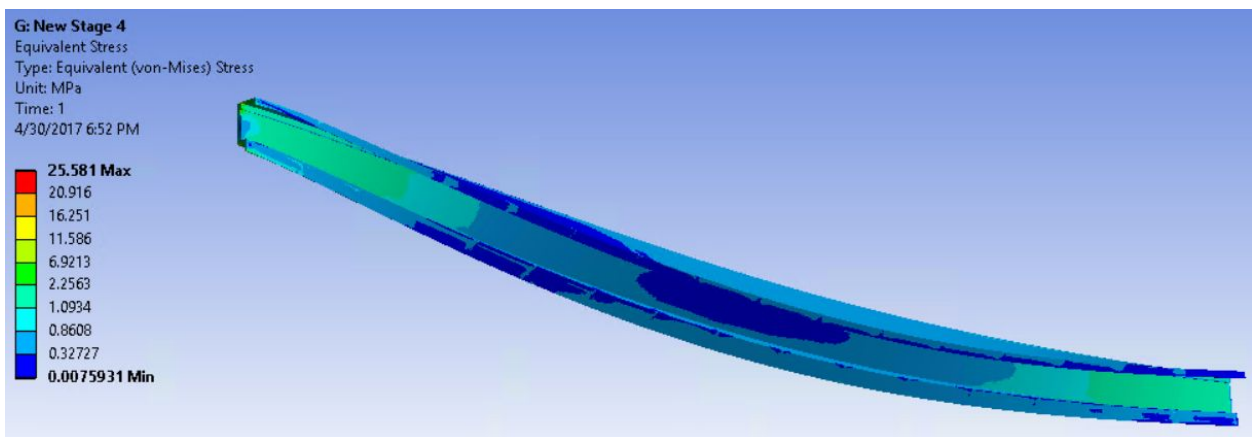


Figure 4.20 Iteration 4 stress results

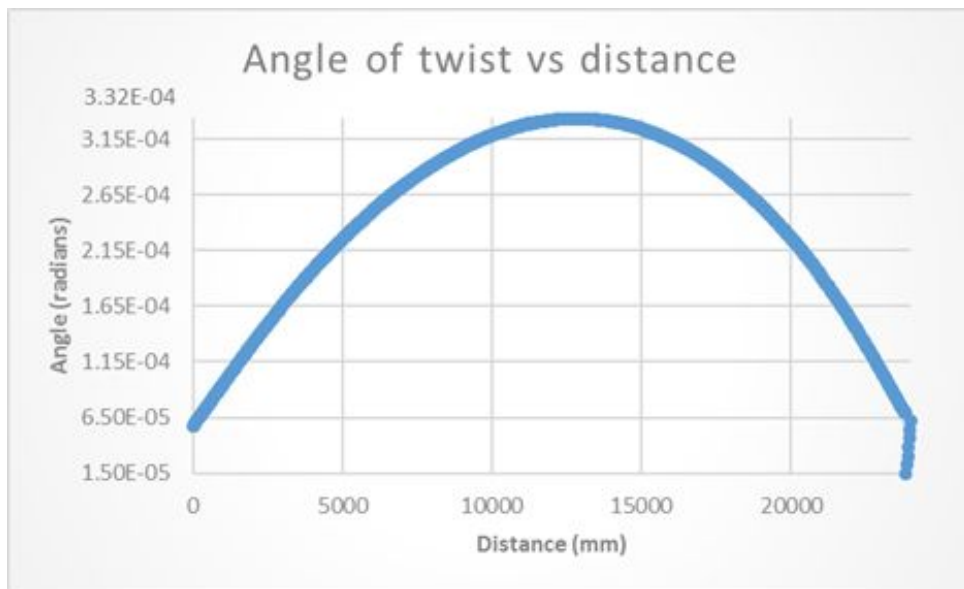
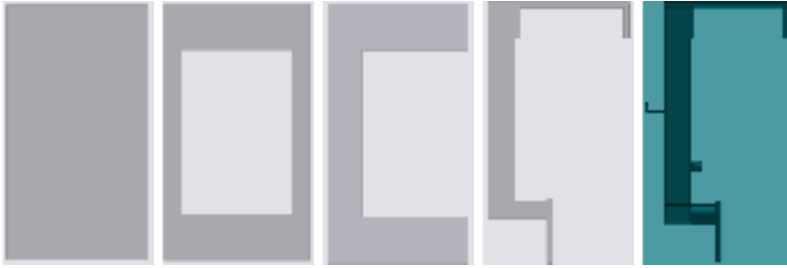


Figure 4.21 iteration 4 twist
 Measure of twist around axis Z for section 4. Maximum angle of twist occurs near midspan.
 Near the end the results become uncorrelated

5.5 Iteration 5 The final profile



For the fifth and final iteration, the geometry was fashioned to replicate the original model, except that every 12th peg in the model had to be removed due to compilation issues (**fig 4.22**). The loadings and support structure were duplicated from iteration 4. The maximum deflection was near 4.35 mm (**fig 4.23**) while the largest stresses were around 2.53 Mpa (**fig 4.24**). The maximum angle of twist was $1.00 * 10^{-2}$ radians (**fig 4.25**)

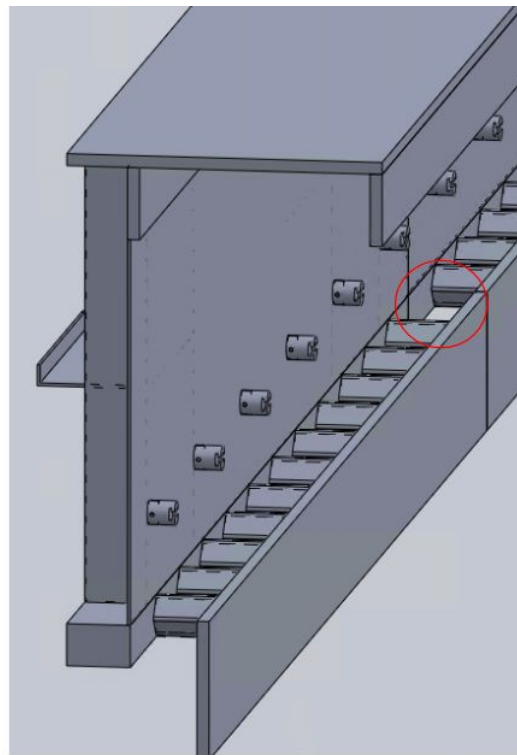


Figure 4.22 Every 12th peg in the model had to be removed due to compilation issues

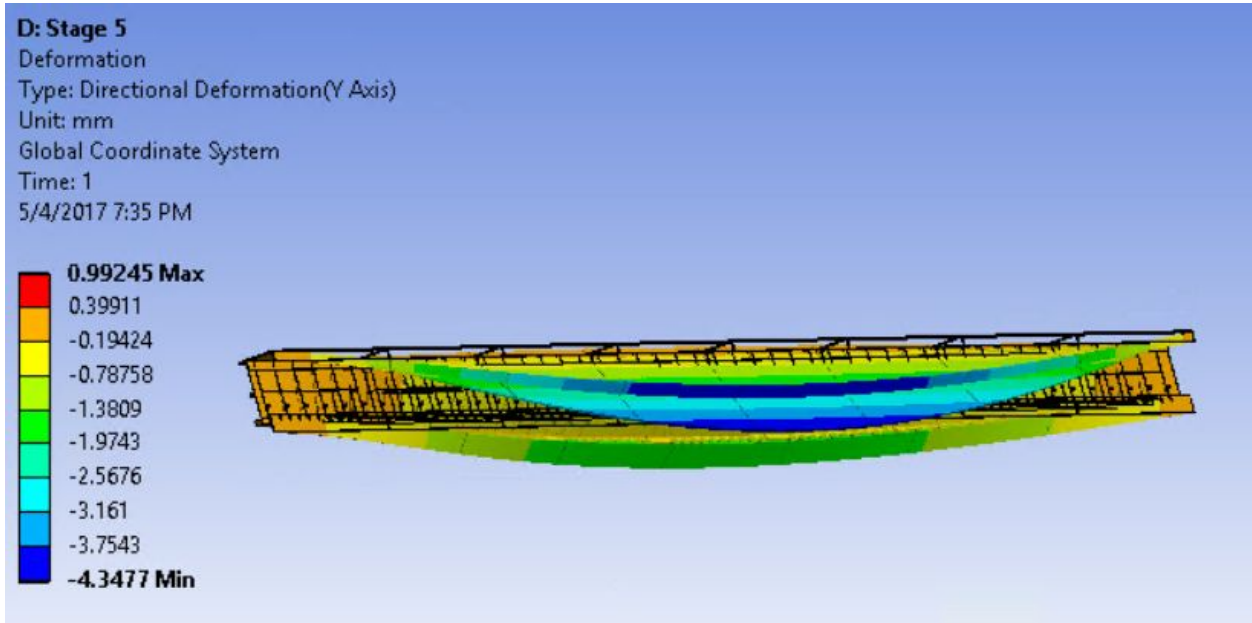


Figure 4.23 Iteration 5 deflection results
 Max deflection takes place at the upper surface flange at midspan

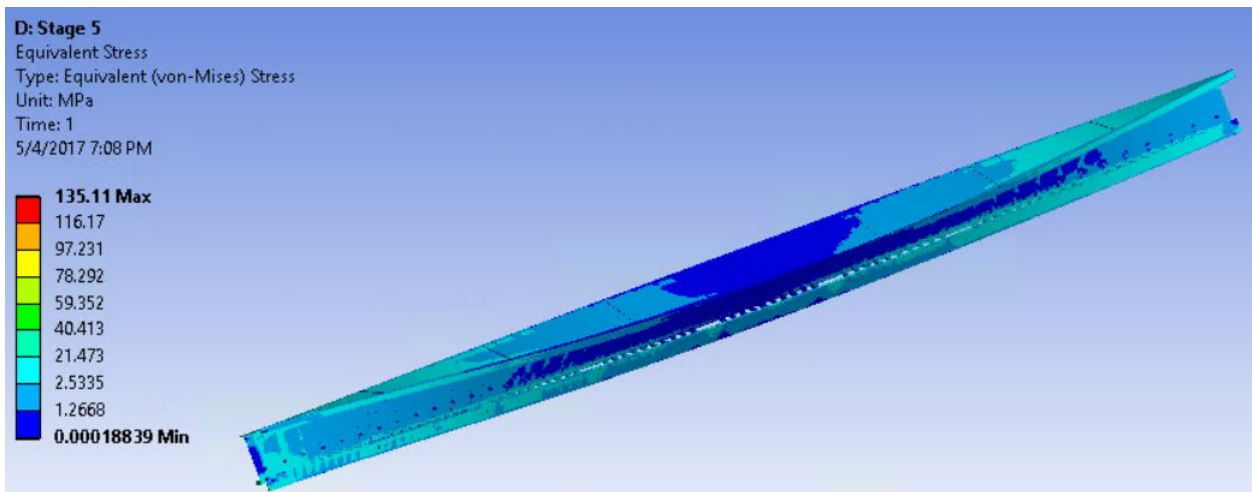


Figure 4.24 Iteration 5 stress results
 Stress is non-uniform due to twisting



Figure 4.25 Iteration 5 graph of twisting
 Measure of twist around axis Z for iteration 5. dx1 and dx2 elements had perfect correlation

5. Conclusion

The deformations of the guideway due to the anticipated loads are safe for public use, with deflection values far smaller than ones found in real world bridges such as Scotland's Forth Road Bridge (Roberts et. all (2012)), far smaller stress values than the Huangpu Bridge in Guangzhou (Wang et. al 2014)

6. Acknowledgements

Before I end this paper, I would like to thank a few people and organizations.

Thank you, Gilles Eggensteiner, Khody Afkhami, and ANSYS inc. for providing me with the software, tutorials, and training needed to perform this project. Your help was indispensable, and none of this could have been done without you

Thank you, Professor Chan for lending your seemingly endless knowledge of finite-element analysis to assist me with this project and for giving me help every time I came over to ask for it.

Thank you, Professor Furman for thinking of this project, assisting me through the research process, and providing priceless feedback for my paper.

Thank, Ron Swenson for pushing my comfort zone and believing in me when this project seemed like it was running into a dead end.

Thank you, Professor Marouf for granting me the opportunity to become a Davidson student scholar

Thank you, Professor McMullin for advising me on the iteration process

Thank you, Mohannad Husain Al-Sherrawi of the University of Baghdad and Chirag Sachdeva of PEC University of Technology for assisting me with the calculating the necessary moment of inertias for parts of the iterations

7. Appendix

A. Derivation of bogie torsional loads

The wind pressure point is located at 1.5 meters below the bottom of the guideway(Gustafsson 2016)

$$\sum F = -F_{lower} + F_{higher} + F_{wind\ on\ bogie} = 0$$

$$\sum M = -x_1 F_{lower} * + x_2 F_{higher} = 0$$

Solving for the moment will give us

$$\rightarrow F_{lower} = \frac{x_2}{x_1} F_{higher}$$

From the CAD model, x_1 was found to be 1.39 meters and x_2 was found to be 2.19 meters (assuming that the forces would be applied at the center of their respected areas) (Fig. 4)

$$\rightarrow F_{lower} = 1.58 F_{higher}$$

The linear force on the bogie would be equal to 766N/m (Gustafsson 2016) and multiplying by 1.5 meters would yield 1149N. Combining this value with the aforementioned moment equation, one would arrive at

$$1.58 F_{higher} + F_{higher} = -1149 N$$

$$F_{lower} = 1981 N$$

And through back substitution, one would logically find that

$$F_{higher} = 3130 N$$

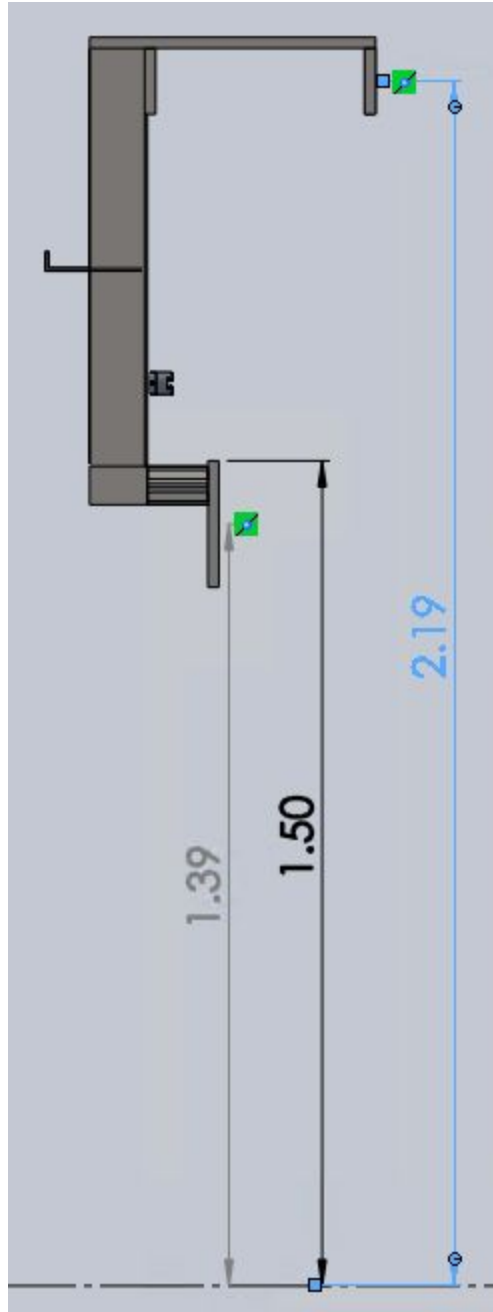


Fig. 6.1 - Distances of the forces from the pressure point

8. References

ANSYS inc. (2013). Case study: Computer simulation improves america's cup yacht (Case study ANSYS inc.

Bhavikatti, S. S. (2014). Introduction. Finite element analysis (). New Delhi: New Age International Pvt.

Furman, B., Fabian, L., Ellis, S., Muller, P., & Swenson, R., 2014. Automated transit networks (ATN): A review of the state of the industry and prospects for the future (No. CA-MTI-14-1227). Available online at: <http://transweb.sjsu.edu/project/1227.html>

Furman, B. J. (2016). The spartan superway: A solar-powered automated transportation network. American Solar Energy Society National Conference 2016, San Francisco.

Gustafsson, B. (2014). In Gustafsson (Ed.), Track and bogie for suspended vehicles. Sweden: US 8807043 B2.

Gustafsson, B. (2016). Beamways track geometry. Linköping: Beamways.

Hua, X. G., Chen, Z. Q., Ni, Y. Q., & Ko, J. M. (2007). Flutter analysis of long-span bridges using ANSYS . Wind and Structures, 10(1), 61-82.

Husain Al-Sherrawi, M, Mohammed, S.M . (2014). The effective width in composite steel concrete beams at ultimate loads . University of Baghdad Engineering Journal, 20(8)

Roberts, G. W., Brown, C. J., Meng, X., Ogunidipe, O., Atkins, C., & Colford, B. (2012). Deflection and frequency monitoring of the forth road bridge, scotland, by GPS. Proceedings of the Institution of Civil Engineers - Bridge Engineering, 165(2), 105-123. doi:10.1680/bren.9.00022

Sachdeva, C., Miglan, J., Padhee, S.S. (2017). Study for effectiveness of idealized theory forFuselage section through finite element analysis. AIAA/ASME/ASCE/AHS/ASC Structures, Structural Dynamics and Materials Conference , Grapevine, Texas. , 58.

Sahroni, T. R. (2015). Modeling and simulation of offshore wind power platform for 5 MW baseline NREL turbine. The Scientific World Journal, 2015

Wang, W., & Liang, J. (2014) Stress measuring and monitoring for main tower of guangzhou pearl river HuangPu bridge doi:10.1117/12.839306 [doi]